S. Garino, P. Antonaci, D. Pastrone, M. Sangermano, F. Maggi
Photo-Polymerization for Additive Manufacturing of Composite Solid Propellants
Acta Astronautica, Vol. 182, 2021, p. 58-65
doi:10.1016/j.actaastro.2021.01.062

Photo-polymerization for additive manufacturing of composite solid propellants

Simone Garino[1], Paola Antonaci[2], Dario Pastrone[3], Marco Sangermano[4], Filippo Maggi[5,*]

Abstract

The established state-of-the-art for composite solid propellant grain manufacture consists in mix-cast-cure process using hazardous chemicals and specific molds for propellant forming. In most of the cases, polyaddition of oligomers involves isocyanate functional groups. Construction constraints limit the feasibility of propellant geometries, confining the pressure-time history of rocket motors to some established configurations. Composition pot-life becomes one of the most important parameters in the definition of correlated industrial processes. An additive manufacturing process for propellant grain production based on UV curing

[*]Corresponding author

Email addresses: d040129@polito.it (Simone Garino), paola.antonaci@polito.it (Paola Antonaci), dario.pastrone@polito.it (Dario Pastrone), marco.sangermano@polito.it (Marco Sangermano), filippo.maggi@polimi.it (Filippo Maggi)

[1]M.Sc. Student, Department of Mechanical and Aerospace Engineering, Politecnico di Torino, Corso Duca degli Abruzzi 24, 10129 Torino, Italy

[2]Assistant Professor, Department of Structural, Geotechnical and Building Engineering, Politecnico di Torino, Corso Duca degli Abruzzi 24, 10129 Torino, Italy

[3]Full Professor, Department of Mechanical and Aerospace Engineering, Politecnico di Torino, Corso Duca degli Abruzzi 24, 10129 Torino, Italy

[4]Associate Professor, Department of Applied Science and Technology, Politecnico di Torino, Corso Duca degli Abruzzi, 24, 10124, Torino, Italy

[5]Associate Professor, Department of Aerospace Science and Technology, Politecnico di Milano, Via La Masa 34, 20156 Milano, Italy

has been recently proposed for patenting. This technique enables more complex grain geometries, paving the way for new propulsive missions, thanks to customized thrust-time profiles or local composition fine tuning. The new curative method makes innovative use of pre-polymers, replacing isocyanates with UV-sensitive components characterized by lower chemical hazard for operators. The paper illustrates the experimental results obtained during the preliminary test campaign on propellant inert simulators, produced as lab-scale proof of concept. The activity targeted mono-layer samples, focusing on binder properties. Dynamic-mechanical thermal analysis, thermal-gravimetric analysis, and stress-strain tests have been carried out to measure mechanical and physical characteristics of different formulations. Both hydroxyl-terminated polybutadiene (HTPB) and polybutadiene diacrylate (PBDDA) binders have been considered, using ammonium sulfate as substitute of ammonium perchlorate. Aluminized and non-aluminized samples have been manufactured to evaluate the impact of opaque-reflective materials during the UV curing process. The reported analyses show comparable results for both the new UV-cured materials and demonstrate the feasibility of propellants based on isocyanate-free process.

Keywords: Composite solid propellant, Polymer binder, HTPB, PBDDA, photopolymerization, Additive manufacturing

---

Photo-polymerization for additive manufacturing of composite solid propellants

Simone Garino[1], Paola Antonaci[2], Dario Pastrone[3], Marco Sangermano[4], Filippo Maggi[5,*]

Nomenclature

Roman symbols

E_t tensile modulus

T_g glass transition temperature

d(0.5) 50th percentile of powder size volume distribution

Greek symbols

*Corresponding author

Email addresses: d040129@polito.it (Simone Garino), paola.antonaci@polito.it (Paola Antonaci), dario.pastrone@polito.it (Dario Pastrone), marco.sangermano@polito.it (Marco Sangermano), filippo.maggi@polimi.it (Filippo Maggi)

[1]M.Sc. Student, Department of Mechanical and Aerospace Engineering, Politecnico di Torino, Corso Duca degli Abruzzi 24, 10129 Torino, Italy

[2]Assistant Professor, Department of Structural, Geotechnical and Building Engineering, Politecnico di Torino, Corso Duca degli Abruzzi 24, 10129 Torino, Italy

[3]Full Professor, Department of Mechanical and Aerospace Engineering, Politecnico di Torino, Corso Duca degli Abruzzi 24, 10129 Torino, Italy

[4]Associate Professor, Department of Applied Science and Technology, Politecnico di Torino, Corso Duca degli Abruzzi, 24, 10124, Torino, Italy

[5]Associate Professor, Department of Aerospace Science and Technology, Politecnico di Milano, Via La Masa 34, 20156 Milano, Italy

σ_m tensile strength

$tan(\delta)$ loss factor

Acronyms

AP ammonium perchlorate

AS ammonium sulfate

ASc coarse ammonium sulfate

ASf fine ammonium sulfate

DMTA dynamic mechanical thermal analysis

HTPB hydroxyl-terminated polybutadiene

PBDDA polybutadiene diacrylate

Phi photo-initiator

phr per hundred rubber

SD_x standard deviation of variable x

SRM solid rocket motor

TGA thermogravimetric analysis

Thiol pentaerythritol tetrakis 3-mercaptopropionate

UV ultraviolet

XCT X-ray computed tomography

1. Introduction

Solid rocket motors are widely used as a source of thrust in many applications, ranging from space launcher boosters to flare and emergency signals. They are often chosen because of high energy density and consequent compactness, operational readiness, technology maturity leading to improved reliability and low cost, as well as long-term storability [1]. In Figure 1 a scheme of a rocket motor is presented. The basic architecture is simple, consisting in a pressure-tight case that contains the propellant, an igniter, and a nozzle. Such SRMs are not throttleable and the thrust-time history is defined by the propellant grain composition (chemical ingredients selected and their percentage), the manufacture process, the nozzle shape and dimensions, and the propellant grain geometry [2].

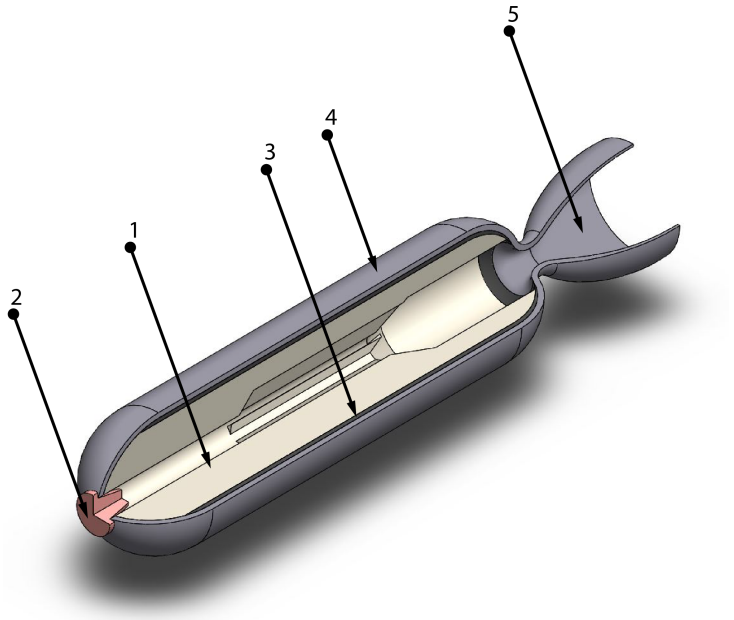

Figure 1: Scheme of a solid rocket motor: 1 = propellant grain, 2 = igniter, 3 = insulation, 4 = motor case body, 5 = nozzle.

Civil and military solid rocket motors (SRMs) commonly adopt composite

propellants. These are heterogeneous energetic materials made by a blend of solid powders, bonded by a polymeric matrix that acts both as structural element and as fuel. Typical ingredients consist of ammonium perchlorate (AP) or other crystalline oxidizers, in the amount of 60 % to 90 % by mass, and aluminum or other light metal alloys acting as high energy density fuel, ranging between 0 % to 20 % of the total. The formulation may include ingredients for combustion tuning called ballistic modifiers (such as burning catalysts, retarding agents, or coolants, in the range of few percent) as well as additives for mixing improvement (plasticizers, wetting agents, curing catalysts) [3].

The binder is often based on hydroxyl terminated polybutadiene (HTPB) which is a viscous liquid pre-polymer. For these applications, its typical molecular weight is about $3000\,\mathrm{g\,mol^{-1}}$ and is commonly cured using isocyanates to form a rubber-like material. The widespread use of HTPB-based binders is motivated by good mechanical properties of final propellant, even in case of compositions characterized by high solid loadings [4, 5]. During preparation, the slurry mixture is castable and propellant grain shape is obtained through the use of molds.

Some papers indicate that optimization of production is one of the key aspects for cost reduction [6, 7]. The desired shape of a solid propellant grain is obtained by means of a process which depends, among the others, by the chemicals used and the grain size. The most common industrial method consists in mixing and casting a slurry based on thermosetting binder. Extrusion is another consolidated option for the production of some categories of thermoplastic energetic materials. The former one consists in a batch process that requires multiple mixes having nominally uniform composition. Advanced continuous techniques are possible also for thermosetting binders. One paper by Thépénier and Fonblanc reports

pilot scale attempts for continuous or semi-continuous mix-cast [6]. The authors describe a study case on Ariane 5 booster production underlining the potential increase of production rate, without specific quantification, though.

The majority of the production facilities are still based on standard mix-cast method, using a forming mandrel to shape the grain. A simplified scheme presented in ref. [1] shows the main manufacturing steps. In a batch production involving inert binder all the ingredients are weighted and premixed, except for the oxidizer and curing agent. This premixed slurry is chemically stable and can be stored till usage. Decantation of solid ingredients can take place and may limit the storage time. Final mixing with oxidizer and curing agent occurs just prior to grain production. The oxidizer is a powder blend containing different particle sizes. Usually bimodal or trimodal size distributions are used for better packing, tuning of ballistic properties, and higher density. The intimate contact between the oxidizer, the binder, and the optional fuel materials (e.g. metal powders) makes the mixture potentially dangerous for fire and explosion risks. The polymerization process starts when adding the curing agent. A typical family of these reactants commonly used in polyurethane binder production consists of isocyanates. They are toxic. The International Agency for Research on Cancer classifies some of them as Group 3 chemical (Not classifiable as to its carcinogenicity to humans) with the exception of toluene di-isocyanate which is listed in Group 2B (Possibly carcinogenic to humans) [8]. However, other studies underline their potential genotoxicity based on experiments in animals [9]. The pot life is the time available between the addition of the curing agent, to the moment the viscosity becomes too high for casting. From an engineering viewpoint, this time frame is identified by reaching threshold values of specific slurry mechanical properties

(i.e. initial viscosity to double, crossing between the real and the imaginary elastic modulus of the material, or limit viscosity value imposed by process). This span is affected by thermal treatment and chemical characteristics of the polymer-curing agent pair, and imposes binding constraints on the possible casting phase duration. The following step consists of pouring of the obtained mixture into the motor case. A mandrel is usually needed to obtain the desired geometry, imposing several restrictions to the final shape, due to de-molding angles, adhesion to the final product, or impossibility of undercut geometry (if not using mechanized or collapsible mandrel). A curing phase in a thermostatic oven follows, that may require several hours. The dimension of the oven is a further constraint that strongly limits the flexibility of the whole manufacture process. Finally, mandrel is extracted. This is a dangerous operation that must be performed gently in order to reduce electrostatic charge accumulation caused by friction with propellant grain. Tooling for shape finalization may be required. Possible defects in the final product consist of any void, bubble or non-homogeneous zone in the grain that could lead to irregular combustion, unpredictable performance, even catastrophic failures. Imperfections are identified in post-production checking with non-destructive controls (i.e. X-ray inspections). It is easy to understand that all the aforementioned issues increase costs making rapid prototyping or testing of a new geometrical configuration a complex task.

In order to improve the grain fabrication process, additive-like deposition of a mixture followed by proper polymerization can be considered. Both deposition and polymerization processes have to be properly developed. A recent patent proposed the deposition of the mixed ingredients followed by a two-step forming process using a combination of two different pre-polymers [10]. The first one is

cured with Ultra Violet (UV) irradiation and grants the shape of the grain. A more classical curing process is used in a second phase to strengthen the mechanical properties thanks to the use of other classical oligomers based on polyaddition (e.g. HTPB). McClain and co-authors demonstrated the ability of a custom additive manufacturing method to print propellants at a high solid loading (85 %) [11]. The paper reported a comparison of two different formulations (HTPB and Illumanbond 60-7105), considering both classical curing process and UV-curing. Reportedly, the UV-curing required 30 minutes of processing time.

The present work refers to a recently proposed fabrication process based on mixture deposition and UV curing [12]. All the typical chemical ingredients are used except for those needed for curing. A proper photo-initiator is introduced instead. The ingredients are mixed and the resulting slurry is continuously deposited. Cross-linking reaction starts immediately thanks to a very fast UV curing process to obtain the final product layer by layer. Once the technological implementation is also finalized, this additive manufacturing procedure is expected to improve the possibility of fabricating complex grain geometries without mandrels, thus contributing to recurrent cost reduction. Moreover, due to the continuous deposition process layer by layer, defects such as voids can be immediately detected and corrective actions can be taken in real time. Due to the new curing process, no ovens are required and the use of noxious isocyanates is avoided. The process can use different pre-polymers with low functionalization, leading to a potential reduction of raw material costs.

The purpose of this paper is to show the results stemming from the initial test campaign carried out to demonstrate the ability of this method to produce solid propellant with proper mechanical and physical characteristics. Focus is posed

on the binder system. Both HTPB and polybutadiene diacrylate (PBDDA) have been used as a binder, adopting a UV-A (390 nm) sensitive catalyst to sensitize them to ultraviolet light. The next sections contain the detailed list of chemical ingredients, experimental set-up, results, comparison, and conclusions.

2. Experiment

2.1. Materials

The materials produced in this work were inert cured slurries that were representative of solid propellant loads. Both non-aluminized and aluminized compositions were manufactured by photo-polymerization, without the use of isocyanates.

2.1.1. Inert replacement of oxidizer

Ammonium sulfate was used instead of solid oxidizer, being a typical choice of inert substitute, as highlighted in a study by Rocketdyne [13]. The mentioned report selects the material mostly on the basis of polymer-bond strength, solubility with other typical ingredients, and interaction with the curing. In this work an additional check ensured similar UV absorption capability of the crystals in the band where the UV-sensitive catalyst operates (in the present case, 390 nm). In this respect, ammonium perchlorate is reportedly transparent to UV, visible, and infrared. The edge of its absorption band is located approximately at 200 nm [14]. Similar behavior was found for the oxidizer substitute. Experimental analyses of the absorption spectrum for ammonium sulfate crystals demonstrate that absorption peaks are not present in the range 200 nm to 900 nm [15].

Ammonium sulfate (minimum purity 99 %) was supplied by Carlo Erba Reagenti. The material was ground and sieved with a planetary ball miller. The particle size was measured through laser diffraction technique using a Malvern Masternsizer

2000. The coarse and fine powder lots featured a d(0.5) of 629 µm and 72.7 µm, respectively.

2.1.2. Binder system based on photo-polymerization

Polymerization requires a photo-initiator, a resin and, optionally, some processing agents such as plasticizers. The photo-initiator is a photo-sensitive component which is converted into a radical by proper illumination. It has the task of triggering and sustaining the reaction of polymerization. In the present work, resins were mixed with 4 phr (per hundred rubber) of Darocur 1173 (2-Hydroxy-2-methylpropiophenone, supplied by BASF). It is photo-sensitive in the UV band and produces a radical-based curing process.

Table 1: Binder systems tested in the paper. Compositions are in mass percent.

Binder Id.	HTPB	PBDDA	Thiol	Phi
H	84.7	0	11.9	3.4
A	0	96.2	0	3.8

Two different binder systems were tested. Their composition is summarized in Table 1. In one case, the polymerization involved PBDDA which is a resin with acrylate functional groups as chain terminators (supplied by Sartomer, SR307). The molecule contains double bonds and requires only a photo-initiator to cure. As a second option, a typical propulsion-grade HTPB was used. This is a pre-polymer with hydroxyl functional groups as chain terminators (PolyBD, R-45, molar mass 2800 g mol^{-1}). Usually, this binder is cured with isocyanates through polyaddition process and it cannot undergo photo-polymerization. Activation of carbon double bonds was obtained by photo-initiation after addition of 14 phr of pentaerythritol tetrakis 3-mercaptopropionate (thiol supplied by Bruno Bock

Chemische Fabrik).

2.1.3. Other additives

Aluminum is a metal fuel used in solid rocket propellants for enhancement of specific impulse and density. Typical particle size spans between 5 µm to 50 µm and powder seems opaque to light. The presence of these particles generates phenomena of UV absorption and scattering, potentially altering the illumination process. For this reason, some formulations incorporated also propulsion-grade micrometric aluminum powders having 30 µm nominal diameter, spherical in shape (supplier Alpoco, Type III).

2.1.4. Samples compositions

Details of tested compositions are shown in Table 2. Compositions H0 and A0 were the reference baselines and were representative of the binder system, without particles (pre-polymer, UV sensitizer, additive). The slurries were composed by 80 % by mass of AS and up to 20 % of binder. Some compositions also included 5 % of aluminum to test the influence of an opaque additive.

Table 2: Composition of samples. Data are in mass percent.

Sample Id.	Binder amount (type)	AS (ASc/ASf)	Al
H0	100 (H)	-	-
H1	20 (H)	80 (100/0)	-
H2	20 (H)	80 (90/10)	-
H3	15 (H)	80 (100/0)	5
H4	15 (H)	80 (90/10)	5
A0	100 (A)	-	-
A1	20 (A)	80 (100/0)	-
A2	20 (A)	80 (90/10)	-
A3	15 (A)	80 (100/0)	5
A4	15 (A)	80 (90/10)	5

2.2. Methods

2.2.1. Samples production procedure

Weighing procedure and chemicals addition was designed to minimize undesired reticulation promoted by natural light, even though the amount of required energy was higher and no effects were expected from direct daylight exposure. Solid and powdered chemicals were quantified, first. Then, liquid chemicals were added in the following order: pre-polymer, additives (if applicable), and UV curing agent. After the preparation phase, a 5 min manual mixing was performed with a spatula to obtain homogeneous mixture. Manual deposition of the final mixture was done on a pre-casted substrate or into a silicon-rubber mold, followed by UV-A (390 nm) irradiation in nitrogen inert gas) for 60 s with 110 $\mathrm{mW\,cm^{-2}}$ UV power. Despite the curing process was based on radical propagation, further tests in open air demonstrated that samples cured successfully also without inert protective atmosphere. As a qualitative example of the current capability, micro-tomography of two multilayer samples are shown in Figure 2. Presence of voids is mainly attributed to the manual deposition process performed at atmospheric pressure.

Samples for this work were mono-layers. Molds for TGA and DMTA shared the same rectangular footprint dimension of $8 \times 20\ \mathrm{mm^2}$. The curing behavior was monitored by changing the deposition thickness ($0.5 - 0.8 - 1.0 - 1.3 - 1.5 - 1.8 - 2.0 - 2.2$mm). For tensile tests, flat dog-bone shaped samples were produced (Fig. 3). Some production issues due to incomplete polymerization were encountered with cylindrical samples 4 mm thick (Fig. 4), especially for those compositions containing metal powders. This issue is caused by failure of UV light penetration in thicker samples and is emphasized by the presence of opaque

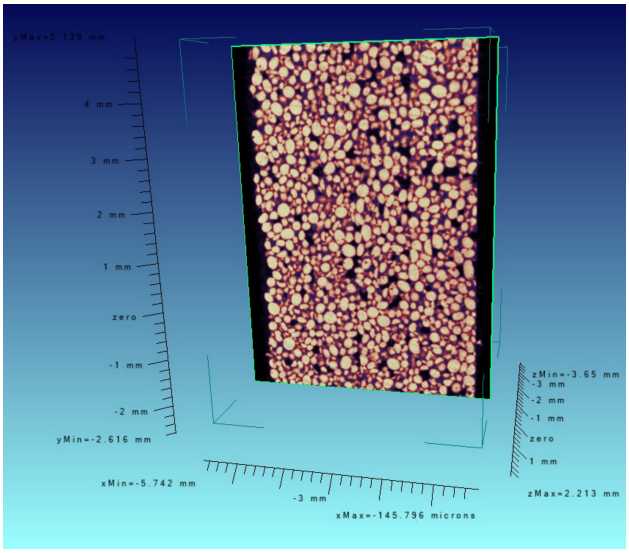

(a) Longtudinal deposition

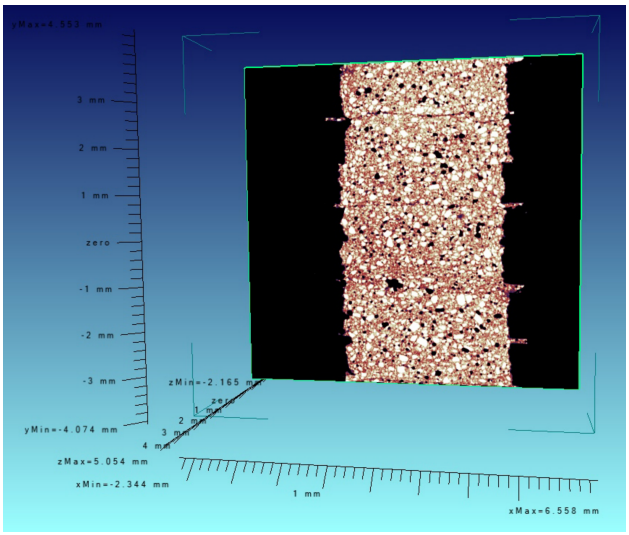

(b) Transverse deposition

Figure 2: Part of multi-layer samples analyzed through XCT. Original size: $4 \times 4 \times 30$ mm^3.

ingredients (i.e. aluminum powder). A review by Decker on photoinitiated polymerization reports that cross-linking propagation is strongly influenced by sample illumination [16]. The paper reports a hyperbolic decrement of radical concentration when UV source is switched off leading to progressive termination of curing propagation.

2.2.2. Thermogravimetric analysis (TGA)

The mass loss of the samples as function of temperature was obtained from TGA, using a TGA/SDTA851^e produced by Mettler Toledo. Constant heating rate of 10 °C min^{-1} from room temperature (about 25 °C) to over 650 °C was used. Nitrogen purging gas flowed at 60 mL min^{-1}. Samples weighted in the range 10 mg to 12 mg. Data obtained from the TGA analysis were manually elaborated using the tangent method to extract reaction onsets.

2.2.3. Dynamic mechanical thermal analysis (DMTA)

Viscoelastic properties of samples as a function of temperature were derived from DMTA analysis. A TT/DMA produced by Triton Technology was used. Samples were subjected to heating from about -80 °C to 20 °C, with a constant rate of 3 °C min^{-1}, while dynamically tested at the reference frequency of 1 Hz. Glass transition temperature was identified monitoring the peak value of loss factor ($\tan(\delta)$, ratio between loss and elastic modulus) during temperature sweep. Considering that T_g cannot be identified as a unique value, the maximum of $\tan\delta$ curve was chosen as reference. Final results were expressed as the average of at least 3 measurements for each sample composition.

2.2.4. Tensile testing

Tensile tests were performed with the aid of an electromechanical testing machine MTS Insight 1 kN Standard, equipped with a load cell of 10 N full-scale.

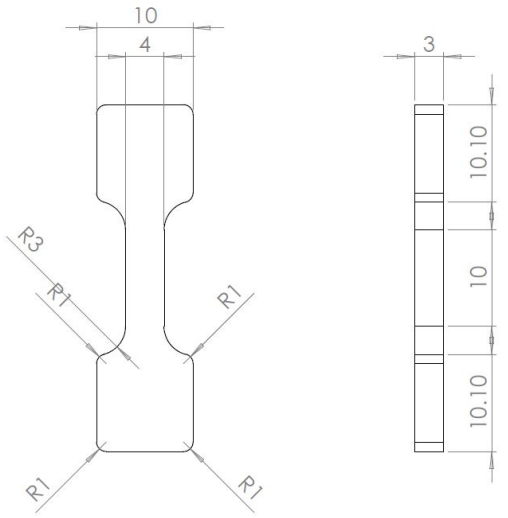

Figure 3: Flat dog-bone sample for tests requiring 12 mm cross section. Measures in mm.

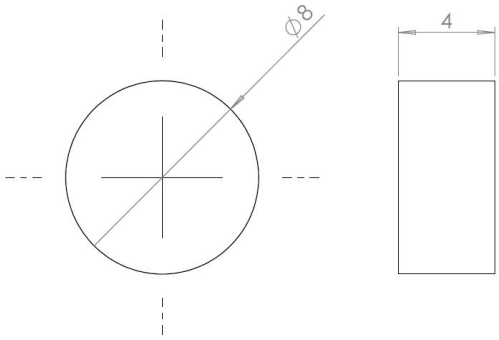

Figure 4: Cylindrical shape and sizes. Measures in mm.

Dog-bone samples of different cross sections were used to allow measurement in the optimal range of the available experimental apparatus, maintaining about 20 % margin from full-scale limit. Cross-section of 12 mm^2 was adopted for samples A0, A1, A2, H0, H1, and H2 whereas 4 mm^2 was used for H3, H4, A3, and A4 materials. This area was measured at the center of the rectilinear part of the flat dog-bone samples. The variation in geometry was obtained by changing the thickness of the mold and keeping the planform shape. Tests were performed at ambient temperature. A constant deformation rate of 5 $mm\,min^{-1}$ was used, with a sampling frequency of 20 Hz. Data were processed to obtain the engineering stress-strain curve and to evaluate main material parameters. Standard deviations were also reported. The value of E_t was calculated by linear interpolation of stress-strain curves in intervals ranging from 10 % to 90 % of the sample maximum stress, discarding data falling in initial and final part of the domain, where non-linear behavior could be manifested.

3. Results and discussion

3.1. TGA results

Figure 5a reports the results for HTPB samples (H series), whereas Figure 5b contains the results for PBDDA samples (A series). Samples H0 and A0 show the decomposition steps of the binder only. The polymers are characterized by an initial low temperature decomposition step where only about $1/5$ of the mass is lost, followed by a high-temperature main reaction, characterized by complete sample gasification. Solid pyrolysis leftovers are about 1 % in mass. The initial onset is very close for the two polymers, being 136 °C for H0 and 140 °C for A0. The end of this decomposition step can be identified at 240 °C for H0 with loss of 22 % and at 251 °C for A0 losing only 17 % of its mass. The H0 sample shows

a slow mass reduction till the beginning of the second and final decomposition at 419 °C, ending at 482 °C. The second decomposition of A0 is more complex. It begins at 430 °C and ends at 487 °C but an intermediate slope change is observed at 454 °C.

The results can be compared with the behavior observed on HTPB propellants cured with isocyanate by Chen and Brill [17]. The literature reference reports a second decomposition step which features the same temperature range of the one recorded in both sample A0 and H0. This reaction is attributed to the vaporization of the butadiene-based pre-polymer, once the cross-link bonds are cleaved. So, the mass loss of samples H0 and A0, preceding the second step, may be associated with the photo-initiation and the correlated chemistry reactions. The comparison between the two polymers shows that PBDDA is characterized by slightly higher thermal stability, compared to HTPB but, globally, their behavior is comparable.

The pattern of the inert slurries (A1 to A4 and H1 to H4) is less significant as the trends of ammonium sulfate and of the polymers overlap. Moreover, the reactivity of the compound is not representative of the final propellant behavior.

3.2. DMTA results

Results of DMTA analyses are reported in Figure 6a for HTPB-based samples, whereas for specimens using PBDDA data are reported in Figure 6b. Obtained data are also gathered in Table 3. The T_g of the original binders are different. The UV-cured HTPB material (H0) features a value which is in line with typical isocyanate-cured polyurethanes that can be found in the range -70 °C to -40 °C, as reported by Desai et al. [18]. The glass transition of the PBDDA polymer is higher. The value measured for the UV-cured pre-polymer (A0) is -22 °C. At authors' knowledge there is not a published reference to compare with. In

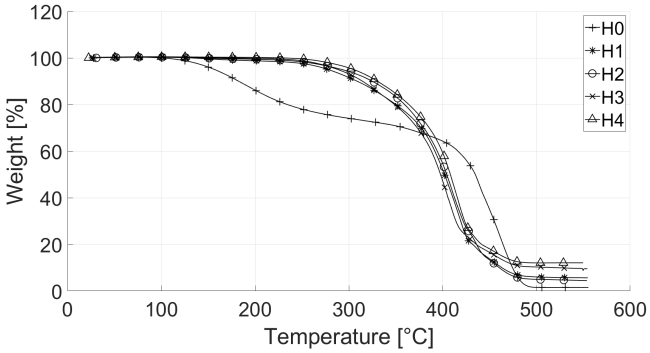

(a) TGA results, HTPB samples

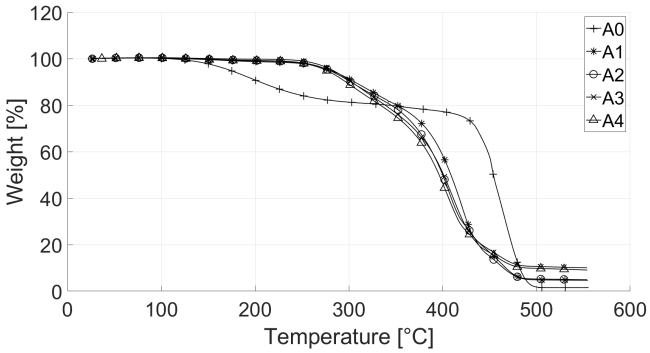

(b) TGA results, PBDDA samples

Figure 5: TGA analysis. Heating rate $10\,^{\circ}\mathrm{C\,min^{-1}}$, nitrogen purging gas flow at $60\,\mathrm{mL\,min^{-1}}$.

both cases, the addition of filler increments the T_g value with respect to the pure polymer, as generally occurs for rubbery binders [19]. The glass transition moves to the range $-35\,^{\circ}\mathrm{C}$ to $-30\,^{\circ}\mathrm{C}$ for HTPB-based material and $-22\,^{\circ}\mathrm{C}$ to $-15\,^{\circ}\mathrm{C}$ for PBDDA-based composite. The peculiar effect of the filler type with each polymer was not in the scope of this work.

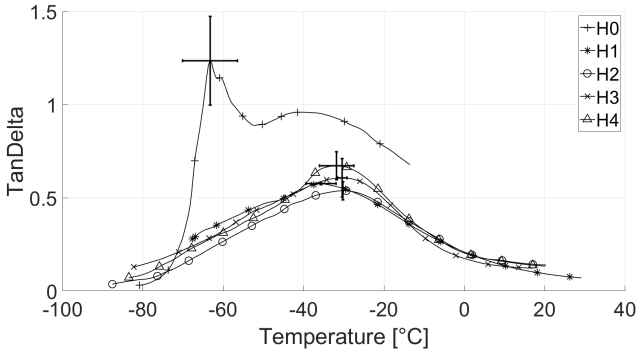

(a) DMTA results, HTPB samples

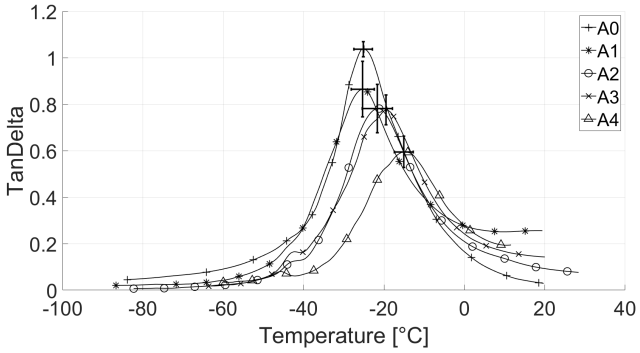

(b) DMTA results, PBDDA samples

Figure 6: DMTA analysis. Heating rate $3\,^{\circ}\mathrm{C\,min^{-1}}$, frequency 1 Hz.

3.3. Tensile test results

Data gathered from tensile test are summarized in Table 4. Average tensile modulus and tensile strength are reported along with their respective standard

Table 3: T_g temperature for each sample family, calculated as average of at least 3 samples

Sample	T_g, °C	SD_{Tg}, °C
H0	-67.2	6.8
H1	-35.0	3.7
H2	-29.6	0.1
H3	-32.7	1.2
H4	-35.2	4.3
A0	-22.4	2.3
A1	-21.7	2.9
A2	-19.5	3.8
A3	-19.1	0.1
A4	-15.2	2.4

deviations, over at least 3 runs. Recorded data and interpolations are displayed in Figure 7 for HTPB-based formulations, whereas PBDDA-based ones are shown in Figure 8.

Both materials tend to show a brittle fracture mode. In general the HTPB-based composition is softer than the PBDDA counterpart. Also with respect to literature reference data, the simulating propellant shows much lower elastic modulus [20]. The strong softening recorded for the HTPB-based composite is caused by the addition of the thiol which is a liquid additive and may promote a plasticization effect. As a consequence, HTPB composition still grants a larger strength at larger strain than the tested PBDDA. Tensile modulus is still too low with respect to standard properties of current propellants but there is still wide margin for targeted optimization. Physical properties of elastomers are strictly connected to cross-link density [21]. Tuning can be obtained through modifications of oligomer molecular weight, branching, presence of double bonds as well as variation of inert diluents, UV irradiation, or photoinitiation strategy.

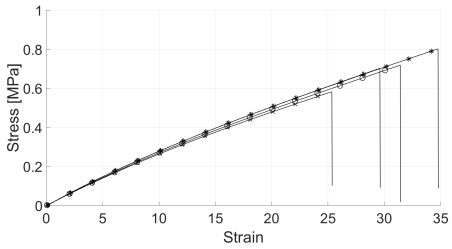

(a) H0 specimens, reference

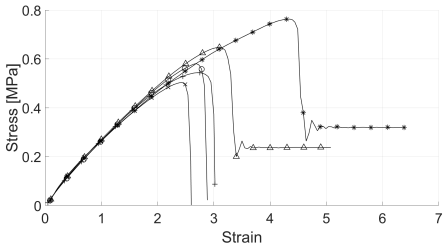

(b) H1 specimens

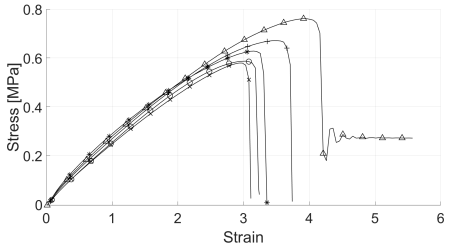

(c) H2 specimens

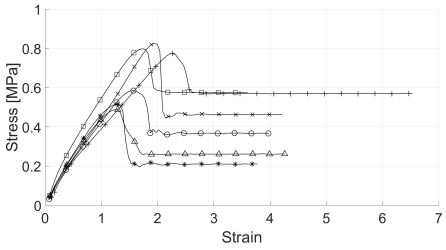

(d) H3 specimens

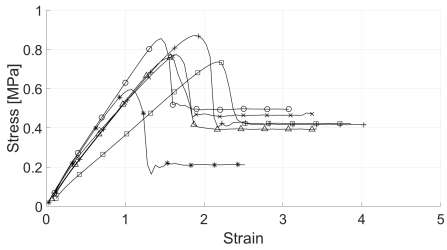

(e) H4 specimens

Figure 7: Tensile tests results for HTPB based specimens. Ambient temperature, deformation rate $5\,\mathrm{mm\,min^{-1}}$.

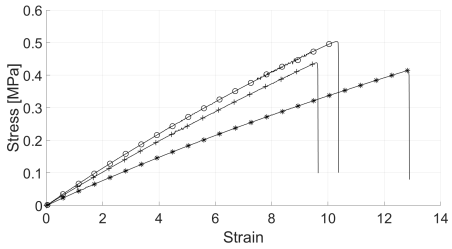

(a) A0 specimens, reference

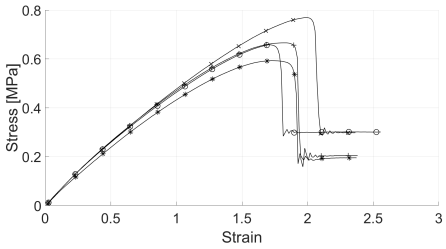

(b) A1 specimens

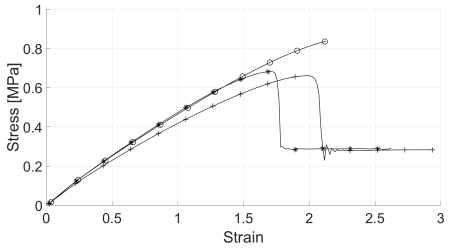

(c) A2 specimens

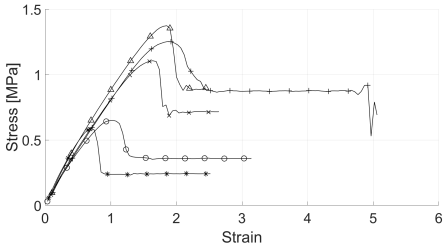

(d) A3 specimens

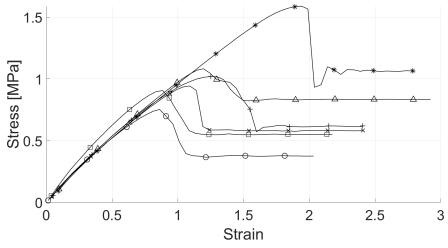

(e) A4 specimens

Figure 8: Tensile tests results for PBDDA based specimens. Ambient temperature, deformation rate 5 mm min^{-1}.

Table 4: Tensile modulus and tensile strength, calculated as average of at least 3 samples for tensile tests

Sample	E_t, MPa	SD_{Et}, MPa	σ_m, MPa	$SD_{\sigma m}$, MPa
H0	0.0225	0.0037	0.7006	0.0908
H1	0.2059	0.0194	0.6076	0.1019
H2	0.2010	0.0044	0.6455	0.0743
H3	0.4049	0.0433	0.6641	0.1520
H4	0.4962	0.0903	0.7652	0.0991
A0	0.0422	0.0089	0.4518	0.0464
A1	0.3845	0.0169	0.6714	0.0729
A2	0.3879	0.0399	0.7262	0.0957
A3	0.7509	0.0812	0.9945	0.3547
A4	0.9075	0.0697	1.0482	0.2876

3.4. Discussion

Both PBDDA and HTPB can be cured by photo-polymerization with both non-metalized and aluminized solid loading. In general, single layers of up to 3 mm did not show problems of incomplete curing. Some issues arose with thickness of 4 mm, becoming evident when aluminum filler was added. PBDDA has the advantage of being photo-sensitive thanks to acrylate functional groups and the sole photo-initiator is enough to trigger the reaction. The hydroxyl functionalization of HTPB is not photo-sensitive so the addition of a thiol containing sulfur activates the carbon double bonds of the polybutadiene resin. The amount of the additive is non-negligible and produces softening of the final products. As consequence, A-series samples are stiffer and hold higher maximum stress than H-series. Rather, HTPB samples hold longer strain. Another reason for the different mechanical properties can be found in the original oligomers. The HTPB resin used in this work is characterized by molar mass of $2800\,\mathrm{g\,mol^{-1}}$ while the SR-307 PBDDA resin is a shorter molecule as it derives from LBH2000, a hydroxyl-terminated

polybutadiene having molar mass of $2000\,\mathrm{g\,mol^{-1}}$ [22, 23]. Regarding the comparison with literature propellant data, the proposed materials are softer, although enabling larger strain at maximum stress and comparable strength [24]. Similar considerations can be done for both monomodal and multimodal slurries. For the HTPB it is interesting to note that the polymerization propagates through radicals and operates on the double bonds of the carbon contained in the butadiene molecule. The hydroxyl functionalization is not involved in the process. The reader should note that equivalent samples cured with isocyanates were not produced in this work because the polymerization process is totally different and a criterion to obtain comparable curing levels was not identified.

Difference between PBDDA and HTPB precursors are shown also by DMTA analyses. The PBDDA-based polymer shows much higher glass transition temperature than HTPB-based rubber. The difference becomes smaller when AS filler is added but the H family still maintains lower T_g. Also this aspect is inherited from the original polymers since the HTPB resin is expected to have a glass transition at $-75\,^{\circ}\mathrm{C}$ while the PBDDA one at $-34\,^{\circ}\mathrm{C}$. With respect to commonly used polymers, the glass transition temperature obtained by the acrylate resin may limit application fields of the polymer in case of extreme storage requirements, due to the risk of grain embrittlement and crack generation.

Finally, from TGA it is possible to observe that both polymers are characterized by similar decomposition steps as they are both based on polybutadiene. Also comparison with published data on isocyanate-cured binders shows similar pyrolysis, granting very low carbon residues.

4. Conclusion

The paper has presented two composite materials based on HTPB and PB-DDA, photo-cured through UV processing. The work demonstrated the feasibility of propellant binder without isocyanates and presented the characterization of a set of compositions filled with ammonium sulfate and aluminum. Despite the products are softer than elastomers currently used in propulsion systems, margin of tailoring is still high, mainly working on cross-link density. Moreover, it is interesting to note that polybutadiene resins without specific functionalization may be used as well, being the double bond of butadiene involved in the radical photo-curing. On the other side, the use of acrylate polymers eases the entire process, being sensitive to UV action.

The proof-of-concept analysis demonstrated that presence of an opaque metal powder does not severely affect the curing procedure. From preliminary tests performed during sample preparation the current thickness limit for 5 % aluminum load seems to be around 3 mm, but specific test campaign should be implemented for accurate determination. In the perspective of developing a method for propellant grain additive manufacturing, this limitation is not critical and represents a processing parameter, even if feasibility studies with higher concentration of opaque ingredients are needed. In this respect, it is expected that the proposed modified compositions and prepolymer proposed, could become an alternative to the actual production process, providing some significant improvements especially for small to medium size grains and prototyping programs, as highlighted also by other literature sources [10, 11]. In addition, new propellant shapes could be obtained, enabling innovative types of propulsion missions.

The evolution of this work will focus primarily on tuning mechanical proper-

ties, processing methods, single/multi-layer deposition techniques, and respective technological implementation. It is not possible to control the curing level in a catalytic process such as in isocyanate-based poly-addition. As consequence, the stiffness of the final propellant should be tailored tuning ingredients and production processes.

References

[1] J.P. Sutton and O. Biblarz, Rocket Propulsion Elements, Seventh Edition, John Wiley and Sons, New York, NY, USA, 2001.

[2] AA.VV., Solid Rocket Motor Performance Analysis and Prediction, NASA Special Publication, SP-8039, 1971

[3] N. Kubota, Energetics of propellants and explosives, In: Propellants and Explosives, Thermochemical Aspects of Combustion, Second Edition, Chapter 4, pp. 69–112, Wiley-VCH, Weinheim, Germany, 2007

[4] A. Davenas, Development of solid modern propellants, Journal of Propulsion and Power, 19(6):1108–1128, 2003

[5] A.K. Mahanta and D.D. Pathak, HTPB-polyurethane: a versatile fuel binder for composite solid propellant, In: Polyurethane, Chapter 11, pp. 229–262, F. Zafar and E. Sharmin Eds., IntechOpen, London, UK, 2012

[6] J. Thépénier and G. Fonblanc, Advanced technologies available for future solid propellant grains, Acta Astronautica, 48(5-12):245–255, 2001

[7] H. Austruy, M. Biagioni, Y. Pelipenko, Improvement in propellant and process for Ariane 5 boosters, AIAA Paper No. 1998-3847, 1998.

[8] Anon. IARC monographs on the identification of carcinogenic hazards to humans, International Agency for Reseach on Cancer, World Health Organization, https://monographs.iarc.fr/agents-classified-by-the-iarc/, last consulted on Dec. 2nd, 2020.

[9] C. Bolognesi, X. Baur, B. Marczynski, H. Norppa, O. Sepai, and G. Sabbioni, Carcinogenic risk of toluene diisocyanate and 4,4′-methylenediphenyl diisocyanate: epidemiological and experimental evidence, Critical Reviews in Toxicology, 31(6):737–772, 2001.

[10] X. Xiangyang, C. Yupeng, L. Han, Z. Wenfang, F. Lixia, and P. Renming, A kind of solid propellant 3D printing and forming method based on ultraviolet light solidification, Patent CN107283826A, 2017

[11] M.S. McClain, I.E. Gunduz, and S.F. Son, Additive manufacturing of ammonium perchlorate composite propellant with high solids loadings. Proceedings of the Combustion Institute, 37(3):3135–3142, 2019.

[12] D. Pastrone, M. Sangermano, S. Garino, and F. Maggi. Composite propellants photopolymerization production. Patent pending, Italian priority number 102019000005788, 2019

[13] AA.VV., Study to find simulants for fuels for use in structures fatigue testing, Technical Report ASD-TRD-63-405, DTIC accession number AD-427123, Air Force Flight Dynamics Laboratory, Research and Technology Division, Air Force Systems Command, OH, 1963.

[14] M.E. Hills and W.R. McBride, Spectral transmittance of single crystal ammonium perchlorate and deuterated ammonium perchlorate, Technical report

NWC TP 5683, DTIC accession number AD-787 504, Naval Weapons Center, China Lake, CA 93555.

[15] B. Xue, H. Huang, M. Mao, and E. Liu, An investigation of the effect of ammonium sulfate addition on compound fertilizer granulation, Particuology, 31:54—58, 2017.

[16] C. Decker, Photoinitiated crosslinking polymerisation, Progress in Polymer Science, 21(4):593–650, 1996.

[17] J.K. Chen and T.B. Brill, Chemistry and kinetics of hydroxyl-terminated polybutadiene (HTPB) and diisocyanate-HTPB polymers during slow decomposition and combustion-like conditions, Combustion and Flames, 87:217–232, 1991.

[18] S. Desai, I.M. Thakore, B.D. Sarawade, and S. Devi, Effect of polyols and diisocyanates on thermo-mechanical and morphological properties of polyurethanes, European Polymer Journal, 36(4):711–725, 2000.

[19] C.G. Robertson, C.J. Lin, M. Rackaitis, and C.M. Roland, Influence of particle size and polymer-filler coupling on viscoelastic glass transition of particle-reinforced polymers, Macromolecules, 41(7):2727–2731, 2008.

[20] A. Göçmez, C. Erisken, Ü. Yilmazer, F. Pekel, and S. Özkar, Mechanical and burning properties of highly loaded composite propellants, Journal of Applied Polymer Science, 67(8):1457–1464, 1997.

[21] L.E. Nielsen, Cross-linking–effect on physical properties of polymers, Journal of Macromolecular Science, Part C, 3(1):69-103, 1969

[22] Anon. Functional additives Poly bd® and Krasol® resins. SMA and Krasol, Downloadable PDF, last download Aug. 15th, 2020.

[23] Anon. Hydroxyl Terminated Polybutadiene Resins and Derivatives - Poly bd® and Krasol®. Cray-Valley website, Doc. id. 3151, 02/10, last download Aug. 15th, 2020.

[24] W.M. Adel and L.G. Zhu, Analysis of mechanical properties for AP/HTPB solid propellant under different loading conditions. International Journal of Aerospace and Mechanical Engineering, 11(12):1915–1919, 2017.